STRUCTURAL CHEMISTRY

ISSN 2053-2296

Crystal structure elucidation of a geminal and vicinal bis(trifluoromethanesulfonate) ester

Thomas Pickl, Julian Zuber, Johannes Stephan and Alexander Pöthig*

School of Natural Sciences & Catalysis Research Center (CRC), Technische Universität München, Ernst-Otto-Fischer Strasse 1, 85748 Garching, Germany. *Correspondence e-mail: alexander.poethig@tum.de

Received 8 April 2024
Accepted 3 June 2024

Edited by T. Ohhara, J-PARC Center, Japan Atomic Energy Agency, Japan

Keywords: crystal structure; bis(trifluoromethanesulfonate); geminal ditriflate; vicinal ditriflate; sensitive oil.

CCDC references: 2360162; 2360161

Supporting information: this article has supporting information at journals.iucr.org/c

Geminal and vicinal bis(trifluoromethanesulfonate) esters are highly reactive alkylene synthons used as potent electrophiles in the macrocyclization of imidazoles and the transformation of bypyridines to diquat derivatives *via* nucleophilic substitution reactions. Herein we report the crystal structures of methylene ($C_3H_2F_6O_6S_2$) and ethylene bis(trifluoromethanesulfonate) ($C_4H_4F_6O_6S_2$), the first examples of a geminal and vicinal bis(trifluoromethanesulfonate) ester characterized by single-crystal X-ray diffraction (SC-XRD). With melting points slightly below ambient temperature, both reported bis(trifluoromethanesulfonate)s are air- and moisture-sensitive oils and were crystallized at 277 K to afford two-component non-merohedrally twinned crystals. The dominant interactions present in both compounds are non-classical C—H···O hydrogen bonds and intermolecular C—F···F—C interactions between trifluoromethyl groups. Molecular electrostatic potential (MEP) calculations by DFT-D3 helped to quantify the polarity between O···H and F···F contacts to rationalize the self-sorting of both bis(trifluoromethanesulfonate) esters in polar (non-fluorous) and non-polar (fluorous) domains within the crystal structure.

1. Introduction

Trifluoromethanesulfonate (triflate) is an important functional group in organic chemistry owing to its strong electron-withdrawing nature (Howells & McCown, 1977; Hendrickson *et al.*, 1977). It is an excellent leaving group used in many organic transformations, such as nucleophilic substitutions, due to the extreme stability of the liberated triflate anion (OTf^-). Thus, the derived triflyl esters (*R*–OTf) are potent electrophiles, representing a halogen-free alternative to alkyl halides in nucleophilic substitution reactions.

Pushing the reactivity of these compounds to an extreme, two triflate groups can be attached to the same carbon to form geminal bis(triflate) esters with the general formula TfO–CR_2–OTf (Martínez *et al.*, 1979, 1987). Among other landmark examples, the parent compound methylene bis(triflate) (**1**, *R* = H) had already been reported in 1980 (Katsuhara & DesMarteau, 1980) but has not been used in chemical synthesis until several decades later. As a highly reactive C1 synthon, the electrophilicity of **1** was eventually harnessed to construct large cyclophanes *via* nucleophilic substitution reactions (Anneser *et al.*, 2015), particularly in cases where bis(imidazoles) were macrocyclized to methylene-bridged tetra(imidazolium) salts (Altmann *et al.*, 2015, 2016; Bernd *et al.*, 2020).

Similarly, the ethylene-bridged bis(triflate) ester TfO–$(CH_2)_2$–OTf (**2**) has been commonly used as a bis-alkylating reagent (C2 synthon), among others, for the transformation of bipyridines to diquat derivatives (Coe *et al.*, 2006) and for the

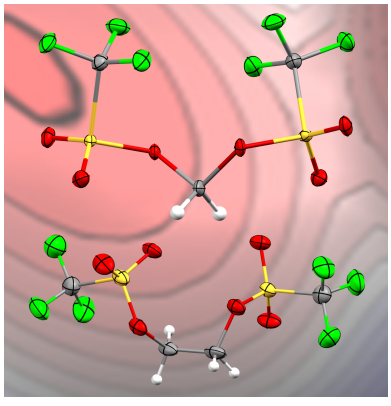

Table 1
Experimental details.

Experiments were carried out at 100 K with Mo $K\alpha$ radiation using a Bruker D8 VENTURE diffractometer. Absorption was corrected for by multi-scan methods (*TWINABS*; Bruker, 2012). H-atom parameters were constrained.

	(**1**)	(**2**)
Crystal data		
Chemical formula	$C_3H_2F_6O_6S_2$	$C_4H_4F_6O_6S_2$
M_r	312.17	326.19
Crystal system, space group	Monoclinic, $P2_1$	Triclinic, $P\overline{1}$
a, b, c (Å)	8.9822 (12), 4.9413 (6), 10.9400 (14)	10.036 (4), 10.664 (3), 11.276 (4)
α, β, γ (°)	90, 102.406 (5), 90	83.540 (9), 64.178 (9), 89.593 (9)
V (Å^3)	474.22 (11)	1078.2 (6)
Z	2	4
μ (mm^{-1})	0.68	0.60
Crystal size (mm)	0.35 × 0.32 × 0.06	0.16 × 0.09 × 0.01
Data collection		
T_{min}, T_{max}	0.540, 0.746	0.564, 0.745
No. of measured, independent and observed [$I > 2\sigma(I)$] reflections	2295, 2295, 2254	4339, 4339, 3403
R_{int}	0.044	0.079
(sin $\theta/\lambda)_{max}$ (Å^{-1})	0.667	0.625
Refinement		
$R[F^2 > 2\sigma(F^2)]$, $wR(F^2)$, S	0.027, 0.072, 1.05	0.066, 0.166, 1.07
No. of reflections	2295	4339
No. of parameters	155	326
No. of restraints	1	0
$\Delta\rho_{max}$, $\Delta\rho_{min}$ (e Å^{-3})	0.41, −0.47	0.60, −0.55
Absolute structure	Flack x determined using 959 quotients $[(I^+) - (I^-)]/[(I^+) + (I^-)]$ (Parsons *et al.*, 2013)	–
Absolute structure parameter	0.12 (4)	–

Computer programs: *APEX4* (Bruker, 2022), *SAINT* (Bruker, 2019), *SHELXT* (Sheldrick, 2015*a*), *SHELXL* (Sheldrick, 2015*b*), *ShelXle* (Hübschle *et al.*, 2011), *PLATON* (Spek, 2020), *enCIFer* (Allen *et al.*, 2004) and *FinalCif* (Kratzert, 2023).

synthesis of ethylene-bridged metal complexes (Lindner *et al.*, 1990) or η^2-olefin metal complexes (Lindner *et al.*, 1985).

Investigating the structure–property relationship of geminal and vicinal bis(sulfonate) esters, such as compounds **1** and **2**, respectively, is imperative to gain a better understanding of their reactivity. In this regard, a structural comparison of similar alkylene bis(mesylates) used as DNA crosslinking agents has been reported, which includes the parent compound MsO–$(CH_2)_2$–OMs (**3**, Ms = mesyl or methanesulfonyl) (McKenna *et al.*, 1989). So far, this study has been complemented by the structural characterizations of only a few other vicinal bis(mesylate) and bis(tosylate) derivatives, such as TsO–$(CH_2)_2$–OTs (**4**, Ts = tosyl or toluenesulfonyl) (Groth *et al.*, 1985), and a handful of geminal bis(tosylates) (Kamal *et al.*, 2020).

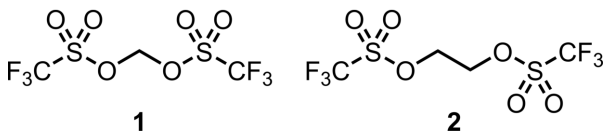

1 **2**

Scheme 1

To date, however, there are no reports on the molecular structures of geminal or vicinal bis(triflate) esters, such as the title compounds **1** and **2** (see Scheme 1). Aiming to study the structure–reactivity relationship of these alkylene sources, we synthesized both compounds and characterized them in the solid state by single-crystal X-ray diffraction (SC-XRD).

2. Experimental

2.1. Synthesis and crystallization

Sulfonate esters **1** and **2** were prepared according to established procedures. Methylene bis(triflate) (**1**) was synthesized by heating an equimolar suspension of triflic anhydride and paraformaldehyde to 353 K, causing the liberation of formaldehyde, which was further reacted with the anhydride at the same temperature for 16 h. Following the evaporation of excess triflic anhydride *in vacuo*, the crude product was passed over a short plug of silica with dichloromethane as the eluent. After removal of all volatiles at 293 K under reduced pressure, analytically pure **1** was obtained as a colourless-to-brown oil. The yields of this reaction typically range between 15 and 20%, which is consistent with previous reports (Anneser *et al.*, 2015).

There are several approaches for the preparation of ethylene bis(triflate) (**2**), *e.g.* the straightforward transmetalation of ethylene dibromide with AgOTf (Shackelford *et al.*, 1985). However, for the purpose of this study, the reaction of ethylene glycol with triflic anhydride under basic conditions was chosen as the preferred method because the diol is readily available and inexpensive, and the desired product is usually obtained in close to quantitative yields (Kuroboshi *et al.*,

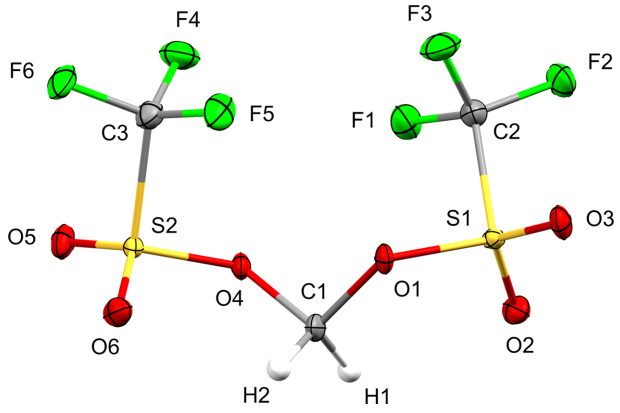

Figure 1
View of methylene bis(trifluoromethanesulfonate) (**1**) with the atom-numbering scheme. Displacement ellipsoids for non-H atoms are drawn at the 30% probability level.

2015). To equimolar amounts of triflic anhydride and pyridine in dichloromethane was added half an equivalent of ethylene glycol at 273 K. The reaction mixture was stirred at the same temperature for 45 min, filtered and washed several times with water. The organic layer was dried over sodium sulfate, filtered and concentrated under reduced pressure. The crude product was filtered over a short plug of silica with dichloromethane as the eluent. All volatiles were subsequently removed at 293 K under reduced pressure to afford analytically pure **2** as a colourless oil (81% yield).

Bis(triflates) **1** and **2** are air- and water-sensitive liquids at ambient temperature, with melting points between 278 and 288 K (Lindner *et al.*, 1981; Anneser *et al.*, 2015). Single crystals were grown by allowing the compounds to solidify slowly over the course of several hours at a temperature of 277 K. To prevent the obtained crystals from melting immediately during picking, the tools used in the process were cooled by repeatedly submerging them in a Dewar flask filled with liquid nitrogen. Additionally, a piece of dry ice was placed on the microscope slide to delay the melting of the specimen on the glass. The selected crystals were then mounted on top of a Kapton micro sample holder (MicroMount) coated with perfluorinated ether and rapidly transferred to the diffractometer.

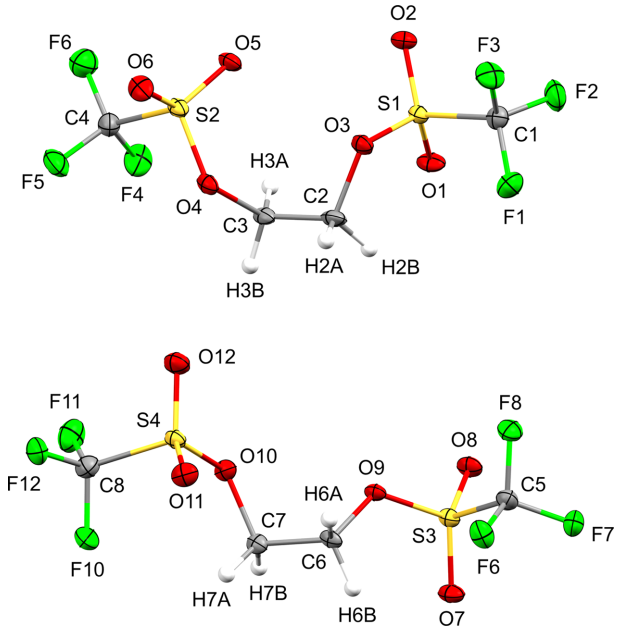

Figure 2
View of both symmetry-independent conformers of ethylene bis(trifluoromethanesulfonate) (**2**) with the atom-numbering scheme. Displacement ellipsoids for non-H atoms are drawn at the 30% probability level.

2.2. Refinement

Data collection and structure refinement details are summarized in Table 1. As implemented in *APEX4* (Bruker, 2022), the non-merohedral twinning of **1** and **2** was addressed by integration of the diffraction data using two orientation matrices in *SAINT* (Bruker, 2019), followed by scaling and absorption correction with *TWINABS* (Bruker, 2012). The structures were solved by *SHELXT* (Sheldrick, 2015*a*) and refined against the respective HKLF5 files using *SHELXL* (Sheldrick, 2015*b*) in conjunction with *ShelXle* (Hübschle *et al.*, 2011). All non-H atoms were refined with anisotropic displacement parameters. H atoms could be located in difference Fourier maps, but for the refinement were positioned geometrically and refined using a riding model, with C—H = 0.99 Å and U_{iso}(H) = 1.2U_{eq}(C).

2.3. DFT calculations

All density functional theory (DFT) calculations were performed with the *ORCA* quantum chemistry package (Version 5.0.4; Neese, 2012, 2022) using the PBE0 exchange-correlation functional (Adamo & Barone, 1999) and the def2-TZVP triple-ξ valence basis set (Weigend & Ahlrichs, 2005), as implemented in *ORCA*. Tighter than normal convergence criteria for SCF calculations (TightSCF) and geometry optimizations (TightOPT) were employed. Grimme's atom-pairwise dispersion correction with the Becke–Johnson damping scheme (D3BJ) was applied to account for dispersion interactions (Grimme *et al.*, 2010, 2011). Geometries were optimized in the gas phase without symmetry constraints. The starting geometries were derived from the SC-XRD structures of **1** and **2**. Frequency analysis at the same level of theory as the geometry optimizations confirmed that the calculations had converged to an energetic minimum. To calculate the molecular electrostatic potentials (MEPs), the total SCF density file obtained after a PBE0/def2-TZVP single-point calculation was first converted to a *Gaussian* cube file using the *orca_plot* module implemented in the *ORCA* package. The MEP was then calculated using the *orca-vpot* module and exported in *Gaussian* cube format. With both cube files in hand, the total SCF density was plotted and the MEP was mapped as a colour onto the isosurface in *Molekel* (Version 4.3; Varetto, 2002).

Table 2
Hydrogen-bond geometry (Å, °) for **1**.

D—H···A	D—H	H···A	D···A	D—H···A
C1—H1···O2	0.99	2.32	2.803 (6)	109
C1—H2···O6	0.99	2.29	2.802 (6)	111
C1—H1···O3^{iii}	0.99	2.51	3.416 (5)	152
C1—H2···O5^{iv}	0.99	2.56	3.430 (5)	147

Symmetry codes: (iii) $-x+2, y-\frac{1}{2}, -z+1$; (iv) $-x+1, y-\frac{1}{2}, -z+1$.

Table 3
Selected interatomic distances (Å) for **1**.

F3···F6^{i}	2.894 (5)	F4···F5^{i}	2.957 (3)
F1···F5^{ii}	2.933 (4)		

Symmetry codes: (i) $-x+1, y-\frac{1}{2}, -z$; (ii) $x, y-1, z$.

3. Results and discussion

Sulfonate esters **1** and **2** both crystallized as two-component non-merohedral twins, and their asymmetric units contain one and two crystallographically independent molecules, respectively (Figs. 1 and 2). Methylene bis(triflate) (**1**) was found to crystallize in the monoclinic space group $P2_1$ (No. 4, Z = 2), and the fractional contribution of the minor twin component was refined to 29% in the final model. Ethylene bis(triflate) (**2**) crystallized in the triclinic space group $P\overline{1}$ (No. 2, Z = 4) with a 37% contribution of the minor twin component. While both triflic esters are achiral in solution, as indicated by a single ^{1}H NMR resonance for the CH_2 protons (Salomon & Salomon, 1979; Katsuhara & DesMarteau, 1980), bis(triflate) **1** appears to be conformationally locked in the solid state and consequently crystallizes in the Sohncke space group $P2_1$. Since sulfur is the heaviest atom of the molecule and molybdenum radiation was used in the diffraction experiment, the absolute structure could only be determined with low accuracy. This is reflected by a Flack parameter of 0.12 with a comparably large standard uncertainty (Flack, 1983; Parsons *et al.*, 2013). In contrast to bis(triflate) **1**, ethylene derivative **2** crystallizes in a centrosymmetric space group ($P\overline{1}$) and the asymmetric unit contains two symmetry-independent conformers of the molecule, which differ mainly in the relative orientation of a triflate group, as expressed by different C—C—O—S torsion angles (Fig. 3). A comparison of the bond distances of both esters reveals almost identical values for chemically equivalent C—F, C—S and terminal S—O bonds, while the average C—O distance is slightly shorter in **1** (1.434 Å) compared to **2** (1.481 Å). In contrast, the mean bond length of the adjacent S—O bond is elongated in **1** (1.573 Å) *versus* **2** (1.547 Å).

The packing of bis(triflates) **1** and **2** is primarily influenced by non-classical C—H···O hydrogen bonds between methylene and sulfonate groups, along with intermolecular C—F···F—C interactions between trifluoromethyl residues closer than the sum of the van der Waals radii (Haynes, 2015) (Tables 2–5). This interaction pattern results in the formation of two-dimensional fluorous and non-fluorous domains in the crystal packing of **1** and **2** (Figs. 4 and 5). Considering this emergence of polar and non-polar domains, we aimed to quantify the influence of differently polarized regions within both structures on the overall solid-state arrangement of the bis(triflates). Therefore, we calculated the molecular electrostatic potentials (MEPs) of **1** and **2** based on the optimized geometries of the respective monomers using DFT-D3 in the gas phase (Fig. 6). As expected, in both cases, the triflate O atoms are the most negatively charged, followed by the F atoms of the CF_3 groups. In stark contrast, the CH_2 fragments of methylene and ethylene bis(triflate) exhibit a high positive charge, which is consistent with their experimentally observed reactivity as strong electrophiles. Along this line, hydrogen-bonding interactions occur only between highly charged parts

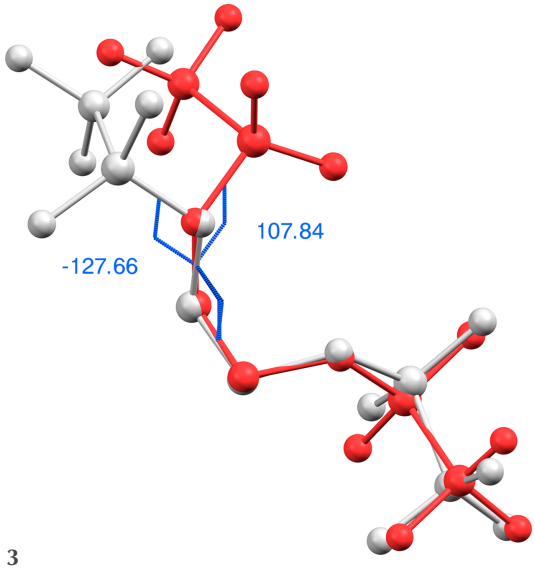

Figure 3
Overlay of the two symmetry-independent conformers of **2**, highlighting the different relative orientations of a trifluoromethanesulfonate group as quantified by different C—C—O—S torsion angles. For clarity, the conformers are drawn in ball-and-stick representation in red and grey, respectively.

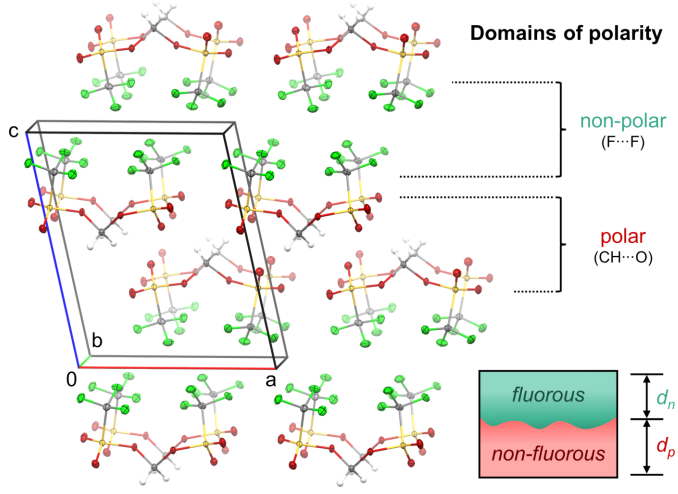

Figure 4
Packing of methylene bis(trifluoromethanesulfonate) (**1**), showing alternating two-dimensional layers of fluorous and non-fluorous domains along the c axis. The share of these domains of different polarity is indicated by the distances d_n and d_p, respectively.

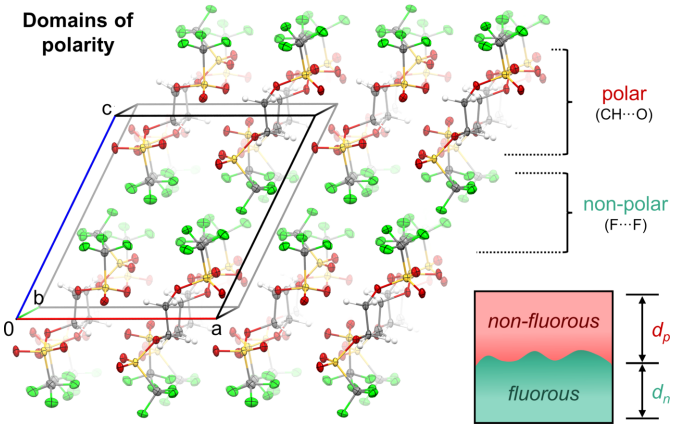

Figure 5
Packing of ethylene bis(trifluoromethanesulfonate) (**2**), showing alternating two-dimensional layers of fluorous and non-fluorous domains along the *c* axis. The share of these domains of different polarity is indicated by the distances d_n and d_p, respectively.

Table 4
Hydrogen-bond geometry (Å, °) for **2**.

D—H···*A*	*D*—H	H···*A*	*D*···*A*	*D*—H···*A*
C2—H2*B*···O8^{i}	0.99	2.62	3.60 (1)	172
C3—H3*A*···O1^{iii}	0.99	2.60	2.984 (9)	103
C3—H3*B*···O1^{iii}	0.99	2.59	2.984 (9)	104
C3—H3*A*···O8^{iv}	0.99	2.59	3.579 (8)	175
C6—H6*A*···O6^{v}	0.99	2.34	3.092 (8)	132
C6—H6*A*···O11^{vi}	0.99	2.47	3.034 (8)	116
C6—H6*B*···O2^{vii}	0.99	2.45	3.210 (8)	133
C7—H7*A*···O5^{vii}	0.99	2.49	3.365 (8)	147
C7—H7*B*···O7^{viii}	0.99	2.70	3.525 (7)	142
C7—H7*B*···O2^{iv}	0.99	2.54	3.349 (9)	139

Symmetry codes: (i) $x, y, z-1$; (iii) $-x+1, -y+1, -z$; (iv) $-x+1, -y+1, -z+1$; (v) $-x+2, -y+1, -z+1$; (vi) $-x+2, -y, -z+2$; (vii) $x, y+1, z-1$; (viii) $-x+1, -y, -z+2$.

Table 5
Selected interatomic distances (Å) for **2**.

F5···F7	2.823 (7)	F3···F9^{ii}	2.954 (5)
F7···F12^{i}	2.951 (7)		

Symmetry codes: (i) $x, y, z-1$; (ii) $-x+2, -y+1, -z$.

of both bis(triflates), namely, positively polarized alkylene H and negatively polarized sulfonate O atoms. The trifluoromethyl groups, with a lower C—F bond polarization, do not participate in hydrogen bonding. Instead, they establish fluorous domains whose arrangement in the crystal is governed by the orientation of the CF_3 groups within the monomers. In methylene bis(triflate) (**1**), these groups align in a shared direction, whereas in ethylene bis(triflate) (**2**), they assume opposite orientations in the molecule. The emerging regions of different polarity within the molecules are thus caused by the observed self-sorting of **1** and **2** into highly polar and nonpolar domains within the crystal structure.

To quantify the share of these alternating domains within the crystal lattice of **1** and **2**, alternating planes parallel to the *ab* plane were defined by (i) all trifluoromethyl C atoms or (ii) all S atoms of each crystallographically independent molecule contained in the unit cell of both structures. Consequently, the separation of polar and non-polar regions was estimated by calculating the distance between two adjacent planes defined by the S atoms (d_p) or C atoms (d_n) for each crystallographically independent molecule (*cf.* Figs. 4 and 5). For compound **2**, the final d_p and d_n values were defined as the average of the individual values of each conformer in the asymmetric unit. For a more detailed definition of the interplanar distances d_p and d_n, see Fig. S1 in the supporting information. In both structures, the polar region was estimated to be larger than the non-polar (compound **1**: $d_p \simeq 3.8$ Å, $d_n \simeq 3.5$ Å; compound **2**: $d_p \simeq 3.7$ Å, $d_n \simeq 2.8$ Å). Interestingly, the determined share of the polar domain in **2** is slightly smaller than in **1**, even though, compared to methylene bis(triflate) (**1**), ethylene congener **2** contains an additional CH_2 group

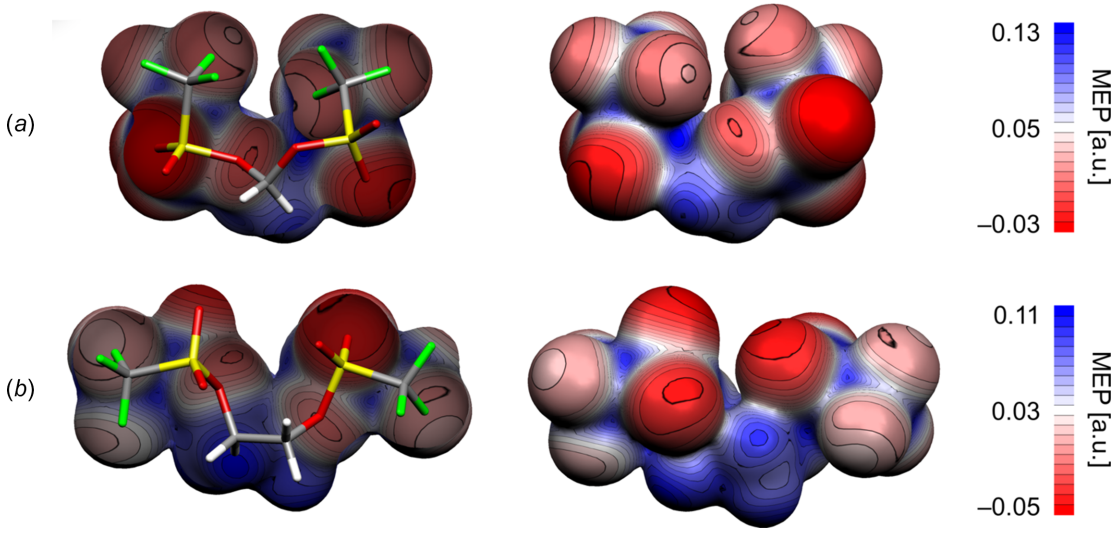

Figure 6
Molecular electrostatic potential (MEP) projected onto the total electron-density surface of (*a*) methylene (**1**) and (*b*) ethylene bis(trifluoromethanesulfonate) (**2**). Geometries are optimized by DFT-D3 at the PBE0/def2-TZVP level of theory and MEPs are shown at 0.0062 a.u. electron density.

acting as a hydrogen-bond donor. Further, the somewhat smaller (polar and non-polar) domain sizes of **2** *versus* **1** suggest tighter packing of ethylene bis(triflate) in general. As an overarching trend, this rough estimation of domain size also indicates that roughly the same share can be attributed to the non-fluorous and fluorous regions in both bis(triflate) structures.

4. Conclusion

The first comprehensive structural analysis of a geminal and vicinal bis(triflate) ester, specifically methylene (**1**) and ethylene bis(triflate) (**2**), is presented. Both compounds are air- and moisture-sensitive oils under ambient conditions and at low temperature crystallized as non-merohedral two-component twins. The crystal structures reveal the presence of non-classical C—H···O hydrogen bonds and intermolecular C—F···F—C interactions, which govern the packing of the compounds in the solid state. Molecular electrostatic potential (MEP) calculations of monomers **1** and **2** based on DFT-D3 showed that these interactions are driven by the high polarity of the O···H contacts and the low polarity of the halogen–halogen contacts, respectively. As a result, bis(triflates) **1** and **2** self-sort in polar (non-fluorous) and non-polar (fluorous) domains of roughly the same relative size within the crystal lattice.

Acknowledgements

This work was financed by the Deutsche Forschungsgemeinschaft (DFG, German Research Foundation). TP thanks the Studienstiftung des deutschen Volkes for a PhD fellowship and associated funding. All authors gratefully acknowledge support from the Fonds der Chemischen Industrie (FCI Sachkostenzuschuss) and the Technical University of Munich (Catalysis Research Center & Graduate School) for financial support. Open access funding enabled and organized by Projekt DEAL.

Funding information

Funding for this research was provided by: Studienstiftung des deutschen Volkes (scholarship to Thomas Pickl); Deutsche Forschungsgemeinschaft (grant No. SPP 1928); Fonds der Chemischen Industrie.

References

Adamo, C. & Barone, V. (1999). *J. Chem. Phys.* **110**, 6158–6170.
Allen, F. H., Johnson, O., Shields, G. P., Smith, B. R. & Towler, M. (2004). *J. Appl. Cryst.* **37**, 335–338.
Altmann, P. J., Jandl, C. & Pöthig, A. (2015). *Dalton Trans.* **44**, 11278–11281.
Altmann, P. J., Weiss, D. T., Jandl, C. & Kühn, F. E. (2016). *Chem. Asian J.* **11**, 1597–1605.
Anneser, M. R., Haslinger, S., Pöthig, A., Cokoja, M., Basset, J.-M. & Kühn, F. E. (2015). *Inorg. Chem.* **54**, 3797–3804.
Bernd, M. A., Dyckhoff, F., Hofmann, B. J., Böth, A. D., Schlagintweit, J. F., Oberkofler, J., Reich, R. M. & Kühn, F. E. (2020). *J. Catal.* **391**, 548–561.
Bruker (2012). *TWINABS*. Bruker AXS Inc., Madison, Wisconsin, USA.
Bruker (2019). *SAINT*. Bruker AXS Inc., Madison, Wisconsin, USA.
Bruker (2022). *APEX4*. Bruker AXS Inc., Madison, Wisconsin, USA.
Coe, B. J., Curati, N. R. M. & Fitzgerald, E. C. (2006). *Synthesis*, pp. 146–150.
Flack, H. D. (1983). *Acta Cryst.* A**39**, 876–881.
Grimme, S., Antony, J., Ehrlich, S. & Krieg, H. (2010). *J. Chem. Phys.* **132**, 154104.
Grimme, S., Ehrlich, S. & Goerigk, L. (2011). *J. Comput. Chem.* **32**, 1456–1465.
Groth, P., Fjellvåg, H., Lehmann, M. S., Tammenmaa, M. & Volden, H. V. (1985). *Acta Chem. Scand. A*, **39**, 587–591.
Haynes, W. M. (2015). In *Chemistry and Physics*, 96th ed. Boca Raton: CRC Press.
Hendrickson, J. B., Sternbach, D. D. & Bair, K. W. (1977). *Acc. Chem. Res.* **10**, 306–312.
Howells, R. D. & McCown, J. D. (1977). *Chem. Rev.* **77**, 69–92.
Hübschle, C. B., Sheldrick, G. M. & Dittrich, B. (2011). *J. Appl. Cryst.* **44**, 1281–1284.
Kamal, R., Kumar, V., Kumar, R., Saini, S. & Kumar, R. (2020). *Synlett*, **31**, 959–964.
Katsuhara, Y. & DesMarteau, D. D. (1980). *J. Fluorine Chem.* **16**, 257–263.
Kratzert, D. (2023). *FinalCif*, https://dkratzert.de/finalcif.html.
Kuroboshi, M., Tanaka, H. & Kondo, T. (2015). *Heterocycles*, **90**, 723–729.
Lindner, E., Pabel, M. & Eichele, K. (1990). *J. Organomet. Chem.* **386**, 187–194.
Lindner, E., Schauss, E., Hiller, W. & Fawzi, R. (1985). *Chem. Ber.* **118**, 3915–3931.
Lindner, E., von Au, G. & Eberle, H.-J. (1981). *Chem. Ber.* **114**, 810–813.
Martínez, A. G., Alvarez, R. M., Fraile, A. G., Subramanian, L. R. & Hanack, M. (1987). *Synthesis*, pp. 49–51.
Martínez, A. G., Ríos, I. E. & Vilar, E. T. (1979). *Synthesis*, pp. 382–383.
McKenna, R., Neidle, S., Kuroda, R. & Fox, B. W. (1989). *Acta Cryst.* C**45**, 311–314.
Neese, F. (2012). *Wiley Interdiscip. Rev. Comput. Mol. Sci.* **2**, 73–78.
Neese, F. (2022). *Wiley Interdiscip. Rev. Comput. Mol. Sci.* **12**, e1606.
Parsons, S., Flack, H. D. & Wagner, T. (2013). *Acta Cryst.* B**69**, 249–259.
Salomon, M. F. & Salomon, R. G. (1979). *J. Am. Chem. Soc.* **101**, 4290–4299.
Shackelford, S. A., Chapman, R. D., Andreshak, J. L., Herrlinger, S. P., Hildreth, R. A. & Smith, J. C. (1985). *J. Fluorine Chem.* **29**, 123.
Sheldrick, G. M. (2015*a*). *Acta Cryst.* A**71**, 3–8.
Sheldrick, G. M. (2015*b*). *Acta Cryst.* C**71**, 3–8.
Spek, A. L. (2020). *Acta Cryst.* E**76**, 1–11.
Varetto, U. (2002). *MOLEKEL*. Version 4.3. Swiss National Supercomputing Centre, Lugano, Switzerland.
Weigend, F. & Ahlrichs, R. (2005). *Phys. Chem. Chem. Phys.* **7**, 3297–3305.

supporting information

Acta Cryst. (2024). C**80**, 278-283 [https://doi.org/10.1107/S2053229624005230]

Crystal structure elucidation of a geminal and vicinal bis(trifluoromethanesulfonate) ester

Thomas Pickl, Julian Zuber, Johannes Stephan and Alexander Pöthig

Computing details

Methanediyl bis(trifluoromethanesulfonate) (1)

Crystal data

$C_3H_2F_6O_6S_2$
M_r = 312.17
Monoclinic, $P2_1$
a = 8.9822 (12) Å
b = 4.9413 (6) Å
c = 10.9400 (14) Å
β = 102.406 (5)°
V = 474.22 (11) Å^3
Z = 2
$F(000)$ = 308
D_x = 2.186 Mg m^{-3}
Melting point: 289 K
Mo $K\alpha$ radiation, λ = 0.71073 Å
Cell parameters from 5142 reflections
θ = 2.3–28.2°
μ = 0.68 mm^{-1}
T = 100 K
Plate, colourless
0.35 × 0.32 × 0.06 mm

Data collection

Bruker D8 VENTURE diffractometer
Radiation source: TXS rotating anode
Helios optic monochromator
Detector resolution: 16 pixels mm^{-1}
ω and φ scans
Absorption correction: multi-scan (TWINABS; Bruker, 2012)
T_{min} = 0.540, T_{max} = 0.746
2295 measured reflections
2295 independent reflections
2254 reflections with $I > 2\sigma(I)$
R_{int} = 0.044
θ_{max} = 28.3°, θ_{min} = 2.3°
h = −11→11
k = −6→6
l = −14→14

Refinement

Refinement on F^2
Least-squares matrix: full
$R[F^2 > 2\sigma(F^2)]$ = 0.027
$wR(F^2)$ = 0.072
S = 1.05
2295 reflections
155 parameters
1 restraint
Primary atom site location: structure-invariant direct methods
Secondary atom site location: difference Fourier map
Hydrogen site location: inferred from neighbouring sites
H-atom parameters constrained
$w = 1/[\sigma^2(F_o^2) + (0.0318P)^2 + 0.3843P]$ where $P = (F_o^2 + 2F_c^2)/3$
$(\Delta/\sigma)_{max}$ < 0.001
$\Delta\rho_{max}$ = 0.41 e Å^{-3}
$\Delta\rho_{min}$ = −0.47 e Å^{-3}
Absolute structure: Flack x determined using 959 quotients [(I+)-(I-)]/[(I+)+(I-)] (Parsons *et al.*, 2013)
Absolute structure parameter: 0.12 (4)

Special details

Experimental. Diffractometer operator T. Pickl scanspeed 1-3 s per frame dx 46 mm 2474 frames measured in 8 data sets phi-scans with delta_phi = 0.5 omega-scans with delta_omega = 0.5 shutterless mode

Geometry. All esds (except the esd in the dihedral angle between two l.s. planes) are estimated using the full covariance matrix. The cell esds are taken into account individually in the estimation of esds in distances, angles and torsion angles; correlations between esds in cell parameters are only used when they are defined by crystal symmetry. An approximate (isotropic) treatment of cell esds is used for estimating esds involving l.s. planes.

Refinement. Refined as a 2-component twin

Fractional atomic coordinates and isotropic or equivalent isotropic displacement parameters (Å²)

	x	*y*	*z*	U_{iso}*/U_{eq}
S1	0.96595 (10)	0.4898 (2)	0.31972 (8)	0.0175 (2)
S2	0.44053 (10)	0.4789 (2)	0.32170 (8)	0.01610 (19)
F1	0.7896 (3)	0.1739 (6)	0.1613 (3)	0.0322 (7)
F2	1.0069 (3)	0.2574 (7)	0.1183 (3)	0.0364 (7)
F3	0.8318 (4)	0.5634 (7)	0.0880 (3)	0.0341 (7)
F4	0.4514 (4)	0.4480 (7)	0.0868 (2)	0.0373 (7)
F5	0.5287 (3)	0.8260 (6)	0.1738 (2)	0.0308 (7)
F6	0.2896 (3)	0.7339 (7)	0.1293 (3)	0.0319 (6)
O1	0.8169 (3)	0.6258 (6)	0.3446 (3)	0.0182 (6)
O2	1.0087 (4)	0.2659 (7)	0.3995 (3)	0.0262 (7)
O3	1.0679 (3)	0.7015 (7)	0.3090 (3)	0.0268 (7)
O4	0.6057 (3)	0.3562 (6)	0.3435 (3)	0.0187 (6)
O5	0.3381 (3)	0.2596 (7)	0.3047 (3)	0.0260 (7)
O6	0.4345 (4)	0.6917 (7)	0.4070 (3)	0.0229 (6)
C1	0.7303 (5)	0.4932 (13)	0.4231 (3)	0.0230 (6)
H1	0.795251	0.361855	0.478791	0.028*
H2	0.691600	0.627764	0.475688	0.028*
C2	0.8932 (5)	0.3618 (10)	0.1609 (4)	0.0229 (9)
C3	0.4270 (5)	0.6309 (9)	0.1666 (4)	0.0229 (8)

Atomic displacement parameters (Å²)

	U^{11}	U^{22}	U^{33}	U^{12}	U^{13}	U^{23}
S1	0.0112 (4)	0.0210 (4)	0.0202 (4)	0.0007 (4)	0.0033 (4)	−0.0024 (5)
S2	0.0115 (4)	0.0185 (4)	0.0186 (4)	0.0011 (5)	0.0038 (3)	0.0015 (5)
F1	0.0281 (15)	0.0359 (16)	0.0334 (13)	−0.0131 (12)	0.0085 (12)	−0.0131 (12)
F2	0.0279 (15)	0.051 (2)	0.0345 (14)	0.0012 (14)	0.0156 (12)	−0.0151 (14)
F3	0.0436 (17)	0.0338 (14)	0.0218 (12)	0.0017 (13)	−0.0001 (12)	0.0042 (10)
F4	0.0454 (17)	0.0465 (19)	0.0206 (11)	0.0085 (17)	0.0083 (11)	−0.0042 (13)
F5	0.0286 (15)	0.0320 (15)	0.0336 (14)	−0.0048 (11)	0.0103 (12)	0.0122 (11)
F6	0.0221 (13)	0.0425 (16)	0.0289 (13)	0.0093 (13)	0.0008 (11)	0.0105 (13)
O1	0.0117 (13)	0.0214 (14)	0.0229 (14)	0.0023 (11)	0.0066 (11)	−0.0006 (11)
O2	0.0246 (16)	0.0269 (17)	0.0266 (15)	0.0108 (14)	0.0043 (13)	0.0047 (13)
O3	0.0188 (15)	0.0306 (17)	0.0331 (16)	−0.0083 (13)	0.0104 (14)	−0.0107 (14)
O4	0.0122 (13)	0.0220 (13)	0.0225 (14)	0.0008 (12)	0.0047 (12)	0.0020 (12)
O5	0.0140 (14)	0.0270 (17)	0.0363 (16)	−0.0021 (12)	0.0036 (13)	0.0039 (14)

O6	0.0212 (15)	0.0249 (15)	0.0228 (14)	0.0065 (13)	0.0049 (12)	0.0000 (13)
C1	0.0121 (13)	0.0387 (19)	0.0182 (13)	−0.0047 (17)	0.0036 (16)	0.000 (2)
C2	0.021 (2)	0.026 (2)	0.0221 (19)	−0.0022 (17)	0.0057 (16)	−0.0054 (17)
C3	0.023 (2)	0.028 (2)	0.0173 (17)	0.0027 (19)	0.0018 (17)	0.0039 (17)

Geometric parameters (Å, º)

S1—O2	1.410 (4)	F2—C2	1.316 (5)
S1—O3	1.412 (4)	F3—C2	1.321 (6)
S1—O1	1.573 (3)	F4—C3	1.308 (5)
S1—C2	1.833 (4)	F5—C3	1.319 (5)
S2—O5	1.408 (3)	F6—C3	1.316 (5)
S2—O6	1.415 (3)	O1—C1	1.435 (5)
S2—O4	1.573 (3)	O4—C1	1.432 (5)
S2—C3	1.835 (4)	C1—H1	0.9900
F1—C2	1.316 (5)	C1—H2	0.9900
F3···F6^{i}	2.894 (5)	F4···F5^{i}	2.957 (3)
F1···F5^{ii}	2.933 (4)		
O2—S1—O3	122.5 (2)	O1—C1—H1	110.1
O2—S1—O1	110.91 (17)	O4—C1—H2	110.1
O3—S1—O1	106.8 (2)	O1—C1—H2	110.1
O2—S1—C2	108.1 (2)	H1—C1—H2	108.5
O3—S1—C2	106.4 (2)	F1—C2—F2	109.2 (4)
O1—S1—C2	99.69 (19)	F1—C2—F3	109.3 (4)
O5—S2—O6	122.87 (19)	F2—C2—F3	109.7 (4)
O5—S2—O4	106.97 (19)	F1—C2—S1	110.4 (3)
O6—S2—O4	110.79 (18)	F2—C2—S1	109.0 (3)
O5—S2—C3	106.3 (2)	F3—C2—S1	109.3 (3)
O6—S2—C3	107.5 (2)	F4—C3—F6	109.9 (4)
O4—S2—C3	99.85 (19)	F4—C3—F5	109.3 (4)
C1—O1—S1	120.0 (3)	F6—C3—F5	109.1 (4)
C1—O4—S2	119.9 (3)	F4—C3—S2	110.3 (3)
O4—C1—O1	107.8 (2)	F6—C3—S2	108.4 (3)
O4—C1—H1	110.1	F5—C3—S2	109.7 (3)
O2—S1—O1—C1	−10.4 (4)	O1—S1—C2—F2	174.9 (3)
O3—S1—O1—C1	−146.1 (3)	O2—S1—C2—F3	170.9 (3)
C2—S1—O1—C1	103.3 (3)	O3—S1—C2—F3	−55.9 (4)
O5—S2—O4—C1	−147.9 (3)	O1—S1—C2—F3	55.0 (3)
O6—S2—O4—C1	−11.6 (4)	O5—S2—C3—F4	−54.8 (4)
C3—S2—O4—C1	101.6 (3)	O6—S2—C3—F4	171.9 (3)
S2—O4—C1—O1	−103.7 (4)	O4—S2—C3—F4	56.3 (4)
S1—O1—C1—O4	−98.6 (4)	O5—S2—C3—F6	65.7 (3)
O2—S1—C2—F1	50.7 (4)	O6—S2—C3—F6	−67.6 (4)
O3—S1—C2—F1	−176.1 (3)	O4—S2—C3—F6	176.7 (3)
O1—S1—C2—F1	−65.2 (4)	O5—S2—C3—F5	−175.3 (3)

O2—S1—C2—F2	−69.3 (4)	O6—S2—C3—F5	51.4 (4)
O3—S1—C2—F2	64.0 (4)	O4—S2—C3—F5	−64.2 (3)

Symmetry codes: (i) −*x*+1, *y*−1/2, −*z*; (ii) *x*, *y*−1, *z*.

Hydrogen-bond geometry (Å, º)

D—H···*A*	*D*—H	H···*A*	*D*···*A*	*D*—H···*A*
C1—H1···O2	0.99	2.32	2.803 (6)	109
C1—H2···O6	0.99	2.29	2.802 (6)	111
C1—H1···O3^{iii}	0.99	2.51	3.416 (5)	152
C1—H2···O5^{iv}	0.99	2.56	3.430 (5)	147

Symmetry codes: (iii) −*x*+2, *y*−1/2, −*z*+1; (iv) −*x*+1, *y*−1/2, −*z*+1.

Ethane-1,2-diyl bis(trifluoromethanesulfonate) (2)

Crystal data

$C_4H_4F_6O_6S_2$
M_r = 326.19
Triclinic, $P\overline{1}$
a = 10.036 (4) Å
b = 10.664 (3) Å
c = 11.276 (4) Å
α = 83.540 (9)°
β = 64.178 (9)°
γ = 89.593 (9)°
V = 1078.2 (6) Å^3
Z = 4
F(000) = 648
D_x = 2.009 Mg m^{-3}
Mo *Kα* radiation, *λ* = 0.71073 Å
Cell parameters from 3670 reflections
θ = 2.3–26.3°
μ = 0.60 mm^{-1}
T = 100 K
Plate, colourless
0.16 × 0.09 × 0.01 mm

Data collection

Bruker D8 VENTURE diffractometer
Radiation source: TXS rotating anode
Helios optic monochromator
Detector resolution: 16 pixels mm^{-1}
ω and *φ* scans
Absorption correction: multi-scan (TWINABS; Bruker, 2012)
T_{min} = 0.564, T_{max} = 0.745
4339 measured reflections
4339 independent reflections
3403 reflections with $I > 2\sigma(I)$
R_{int} = 0.079
θ_{max} = 26.4°, θ_{min} = 1.9°
h = −11→12
k = −13→13
l = 0→14

Refinement

Refinement on F^2
Least-squares matrix: full
$R[F^2 > 2\sigma(F^2)]$ = 0.066
$wR(F^2)$ = 0.166
S = 1.07
4339 reflections
326 parameters
0 restraints
Primary atom site location: structure-invariant direct methods
Secondary atom site location: difference Fourier map
Hydrogen site location: inferred from neighbouring sites
H-atom parameters constrained
$w = 1/[\sigma^2(F_o^2) + (0.0356P)^2 + 5.6794P]$ where $P = (F_o^2 + 2F_c^2)/3$
$(\Delta/\sigma)_{max} < 0.001$
$\Delta\rho_{max}$ = 0.60 e Å^{-3}
$\Delta\rho_{min}$ = −0.55 e Å^{-3}

Special details

Experimental. Diffractometer operator T. Pickl scanspeed 5-10 s per frame dx 62 mm 1944 frames measured in 7 data sets phi-scans with delta_phi = 0.5 omega-scans with delta_omega = 0.5 shutterless mode

Geometry. All esds (except the esd in the dihedral angle between two l.s. planes) are estimated using the full covariance matrix. The cell esds are taken into account individually in the estimation of esds in distances, angles and torsion angles; correlations between esds in cell parameters are only used when they are defined by crystal symmetry. An approximate (isotropic) treatment of cell esds is used for estimating esds involving l.s. planes.

Refinement. Refined as a 2-component twin.

Fractional atomic coordinates and isotropic or equivalent isotropic displacement parameters (Å²)

	x	*y*	*z*	U_{iso}*/U_{eq}
C1	0.7390 (7)	0.7806 (7)	−0.3145 (7)	0.0305 (15)
C2	0.7981 (8)	0.5426 (6)	−0.0952 (8)	0.0330 (16)
H2A	0.902806	0.520173	−0.141213	0.040*
H2B	0.739825	0.497232	−0.130181	0.040*
C3	0.7408 (7)	0.5038 (6)	0.0505 (7)	0.0269 (14)
H3A	0.642752	0.539256	0.098399	0.032*
H3B	0.728878	0.410543	0.069459	0.032*
C4	0.7031 (9)	0.5807 (7)	0.3481 (7)	0.0361 (17)
C5	0.8589 (8)	0.2726 (6)	0.6257 (7)	0.0302 (14)
C6	0.7927 (7)	0.0998 (5)	0.9138 (6)	0.0221 (13)
H6A	0.899447	0.113447	0.889450	0.027*
H6B	0.782152	0.034746	0.862035	0.027*
C7	0.7111 (7)	0.0564 (6)	1.0578 (6)	0.0241 (13)
H7A	0.753362	−0.021922	1.080005	0.029*
H7B	0.605728	0.037346	1.080766	0.029*
C8	0.7390 (8)	0.0661 (7)	1.3534 (7)	0.0357 (17)
O1	0.5416 (5)	0.6374 (4)	−0.1115 (5)	0.0314 (11)
O2	0.6156 (5)	0.8470 (4)	−0.0780 (5)	0.0280 (10)
O3	0.7869 (5)	0.6800 (4)	−0.1208 (5)	0.0273 (10)
O4	0.8474 (5)	0.5512 (4)	0.0961 (5)	0.0271 (10)
O5	0.7148 (5)	0.7467 (4)	0.1546 (5)	0.0293 (10)
O6	0.9481 (5)	0.7020 (5)	0.1759 (5)	0.0378 (12)
O7	0.6265 (5)	0.1192 (4)	0.7537 (5)	0.0321 (11)
O8	0.6023 (5)	0.3478 (4)	0.7861 (5)	0.0294 (10)
O9	0.7323 (4)	0.2186 (4)	0.8829 (4)	0.0220 (9)
O10	0.7222 (5)	0.1561 (4)	1.1360 (4)	0.0269 (10)
O11	0.9608 (5)	0.0795 (4)	1.1190 (5)	0.0321 (11)
O12	0.8618 (5)	0.2776 (4)	1.2118 (5)	0.0358 (12)
F1	0.7956 (5)	0.6816 (4)	−0.3792 (4)	0.0465 (11)
F2	0.6383 (5)	0.8273 (4)	−0.3533 (5)	0.0492 (12)
F3	0.8467 (5)	0.8687 (4)	−0.3484 (4)	0.0440 (11)
F4	0.5908 (5)	0.5129 (4)	0.3503 (4)	0.0496 (12)
F5	0.7841 (6)	0.5051 (4)	0.3855 (5)	0.0506 (12)
F6	0.6486 (6)	0.6642 (5)	0.4320 (5)	0.0556 (13)
F7	0.8389 (5)	0.2819 (4)	0.5157 (4)	0.0397 (10)
F8	0.9190 (4)	0.3805 (4)	0.6300 (4)	0.0357 (9)

F9	0.9521 (4)	0.1820 (4)	0.6202 (4)	0.0363 (10)
F10	0.6861 (6)	−0.0449 (4)	1.3420 (5)	0.0580 (14)
F11	0.6265 (5)	0.1269 (5)	1.4300 (4)	0.0518 (12)
F12	0.8276 (6)	0.0428 (4)	1.4110 (4)	0.0480 (12)
S1	0.65129 (17)	0.73351 (14)	−0.13709 (15)	0.0212 (3)
S2	0.81148 (18)	0.66163 (14)	0.18055 (17)	0.0247 (4)
S3	0.68116 (17)	0.23493 (14)	0.77089 (16)	0.0227 (3)
S4	0.84046 (18)	0.15361 (14)	1.18972 (16)	0.0237 (3)

Atomic displacement parameters (Å²)

	U^{11}	U^{22}	U^{33}	U^{12}	U^{13}	U^{23}
C1	0.026 (4)	0.032 (4)	0.033 (4)	0.000 (3)	−0.014 (3)	−0.004 (3)
C2	0.038 (4)	0.018 (3)	0.055 (5)	0.011 (3)	−0.029 (4)	−0.012 (3)
C3	0.028 (3)	0.017 (3)	0.046 (4)	0.000 (2)	−0.026 (3)	−0.005 (3)
C4	0.047 (4)	0.032 (4)	0.036 (4)	0.000 (3)	−0.025 (4)	−0.002 (3)
C5	0.036 (4)	0.024 (3)	0.032 (4)	0.006 (3)	−0.017 (3)	−0.005 (3)
C6	0.019 (3)	0.016 (3)	0.034 (4)	0.003 (2)	−0.015 (3)	−0.001 (2)
C7	0.021 (3)	0.024 (3)	0.032 (3)	0.000 (3)	−0.016 (3)	−0.001 (3)
C8	0.039 (4)	0.037 (4)	0.035 (4)	−0.002 (3)	−0.020 (4)	−0.005 (3)
O1	0.023 (2)	0.021 (2)	0.051 (3)	−0.0051 (18)	−0.016 (2)	−0.005 (2)
O2	0.027 (2)	0.019 (2)	0.035 (3)	0.0015 (18)	−0.010 (2)	−0.0048 (19)
O3	0.026 (2)	0.023 (2)	0.038 (3)	0.0038 (18)	−0.019 (2)	−0.0024 (19)
O4	0.025 (2)	0.022 (2)	0.042 (3)	0.0004 (17)	−0.022 (2)	0.0003 (19)
O5	0.031 (3)	0.019 (2)	0.043 (3)	0.0054 (18)	−0.021 (2)	−0.0015 (19)
O6	0.032 (3)	0.034 (3)	0.056 (3)	−0.011 (2)	−0.029 (3)	0.002 (2)
O7	0.034 (3)	0.022 (2)	0.049 (3)	−0.0020 (19)	−0.026 (2)	−0.005 (2)
O8	0.028 (2)	0.021 (2)	0.042 (3)	0.0086 (18)	−0.019 (2)	−0.0056 (19)
O9	0.022 (2)	0.016 (2)	0.028 (2)	0.0027 (16)	−0.0114 (19)	−0.0034 (17)
O10	0.029 (2)	0.025 (2)	0.036 (3)	0.0092 (18)	−0.022 (2)	−0.0071 (19)
O11	0.024 (2)	0.034 (3)	0.044 (3)	0.0098 (19)	−0.019 (2)	−0.011 (2)
O12	0.040 (3)	0.026 (2)	0.046 (3)	0.005 (2)	−0.023 (3)	−0.004 (2)
F1	0.055 (3)	0.048 (3)	0.036 (2)	0.008 (2)	−0.018 (2)	−0.015 (2)
F2	0.057 (3)	0.059 (3)	0.045 (3)	0.013 (2)	−0.035 (2)	−0.002 (2)
F3	0.043 (3)	0.037 (2)	0.038 (2)	−0.0109 (19)	−0.008 (2)	0.0069 (19)
F4	0.047 (3)	0.055 (3)	0.037 (2)	−0.023 (2)	−0.012 (2)	0.009 (2)
F5	0.067 (3)	0.036 (2)	0.053 (3)	−0.002 (2)	−0.034 (3)	0.012 (2)
F6	0.072 (3)	0.049 (3)	0.042 (3)	0.005 (2)	−0.020 (3)	−0.007 (2)
F7	0.055 (3)	0.040 (2)	0.026 (2)	0.001 (2)	−0.020 (2)	−0.0021 (17)
F8	0.034 (2)	0.033 (2)	0.036 (2)	−0.0097 (17)	−0.0120 (19)	−0.0011 (17)
F9	0.030 (2)	0.036 (2)	0.032 (2)	0.0125 (17)	−0.0056 (18)	−0.0003 (17)
F10	0.091 (4)	0.040 (3)	0.040 (3)	−0.030 (3)	−0.029 (3)	0.010 (2)
F11	0.040 (3)	0.072 (3)	0.035 (2)	−0.001 (2)	−0.008 (2)	−0.009 (2)
F12	0.072 (3)	0.038 (3)	0.045 (3)	−0.001 (2)	−0.038 (3)	0.006 (2)
S1	0.0196 (7)	0.0175 (7)	0.0266 (8)	0.0005 (6)	−0.0106 (6)	−0.0014 (6)
S2	0.0257 (8)	0.0193 (7)	0.0330 (9)	−0.0026 (6)	−0.0173 (7)	0.0012 (6)
S3	0.0206 (7)	0.0188 (7)	0.0317 (8)	0.0019 (6)	−0.0145 (7)	−0.0024 (6)
S4	0.0251 (8)	0.0184 (7)	0.0301 (8)	0.0030 (6)	−0.0147 (7)	−0.0013 (6)

Geometric parameters (Å, º)

C1—F3	1.331 (8)	C7—O10	1.489 (7)
C1—F1	1.332 (8)	C8—F11	1.308 (9)
C1—F2	1.337 (8)	C8—F12	1.318 (8)
C1—S1	1.810 (7)	C8—F10	1.342 (8)
C2—O3	1.474 (7)	C8—S4	1.817 (8)
C2—C3	1.493 (10)	O1—S1	1.420 (4)
C3—O4	1.487 (7)	O2—S1	1.416 (4)
C4—F5	1.305 (8)	O3—S1	1.548 (4)
C4—F6	1.311 (9)	O4—S2	1.540 (5)
C4—F4	1.332 (8)	O5—S2	1.423 (4)
C4—S2	1.831 (8)	O6—S2	1.417 (5)
C5—F8	1.318 (8)	O7—S3	1.420 (4)
C5—F9	1.327 (8)	O8—S3	1.421 (4)
C5—F7	1.334 (8)	O9—S3	1.551 (4)
C5—S3	1.828 (7)	O10—S4	1.549 (4)
C6—O9	1.473 (7)	O11—S4	1.417 (5)
C6—C7	1.483 (9)	O12—S4	1.407 (5)
F5···F7	2.823 (7)	F3···F9^{ii}	2.954 (5)
F7···F12^{i}	2.951 (7)		
F3—C1—F1	108.8 (6)	C2—O3—S1	120.5 (4)
F3—C1—F2	108.5 (6)	C3—O4—S2	121.4 (4)
F1—C1—F2	107.9 (6)	C6—O9—S3	121.4 (4)
F3—C1—S1	111.3 (5)	C7—O10—S4	121.4 (4)
F1—C1—S1	110.6 (5)	O2—S1—O1	121.9 (3)
F2—C1—S1	109.6 (5)	O2—S1—O3	108.4 (3)
O3—C2—C3	109.8 (5)	O1—S1—O3	112.0 (3)
O4—C3—C2	108.9 (5)	O2—S1—C1	105.9 (3)
F5—C4—F6	109.2 (6)	O1—S1—C1	107.1 (3)
F5—C4—F4	108.6 (6)	O3—S1—C1	98.9 (3)
F6—C4—F4	108.5 (7)	O6—S2—O5	122.7 (3)
F5—C4—S2	111.3 (5)	O6—S2—O4	105.6 (3)
F6—C4—S2	109.7 (5)	O5—S2—O4	112.3 (3)
F4—C4—S2	109.5 (5)	O6—S2—C4	106.2 (3)
F8—C5—F9	108.6 (6)	O5—S2—C4	106.0 (3)
F8—C5—F7	108.5 (5)	O4—S2—C4	101.8 (3)
F9—C5—F7	108.8 (6)	O7—S3—O8	123.2 (3)
F8—C5—S3	111.2 (5)	O7—S3—O9	112.2 (3)
F9—C5—S3	110.0 (4)	O8—S3—O9	106.4 (3)
F7—C5—S3	109.6 (5)	O7—S3—C5	106.0 (3)
O9—C6—C7	109.1 (5)	O8—S3—C5	105.9 (3)
C6—C7—O10	110.0 (5)	O9—S3—C5	100.5 (3)
F11—C8—F12	108.9 (6)	O12—S4—O11	122.1 (3)
F11—C8—F10	107.7 (6)	O12—S4—O10	107.5 (3)
F12—C8—F10	108.1 (6)	O11—S4—O10	111.9 (3)

F11—C8—S4	112.1 (5)	O12—S4—C8	105.7 (3)
F12—C8—S4	110.2 (5)	O11—S4—C8	106.3 (3)
F10—C8—S4	109.6 (5)	O10—S4—C8	101.1 (3)

Symmetry codes: (i) *x*, *y*, *z*−1; (ii) −*x*+2, −*y*+1, −*z*.

Hydrogen-bond geometry (Å, º)

D—H···*A*	*D*—H	H···*A*	*D*···*A*	*D*—H···*A*
C2—H2*B*···O8^{i}	0.99	2.62	3.60 (1)	172
C3—H3*A*···O1^{iii}	0.99	2.60	2.984 (9)	103
C3—H3*B*···O1^{iii}	0.99	2.59	2.984 (9)	104
C3—H3*A*···O8^{iv}	0.99	2.59	3.579 (8)	175
C6—H6*A*···O6^{v}	0.99	2.34	3.092 (8)	132
C6—H6*A*···O11^{vi}	0.99	2.47	3.034 (8)	116
C6—H6*B*···O2^{vii}	0.99	2.45	3.210 (8)	133
C7—H7*A*···O5^{vii}	0.99	2.49	3.365 (8)	147
C7—H7*B*···O7^{viii}	0.99	2.70	3.525 (7)	142
C7—H7*B*···O2^{iv}	0.99	2.54	3.349 (9)	139

Symmetry codes: (i) *x*, *y*, *z*−1; (iii) −*x*+1, −*y*+1, −*z*; (iv) −*x*+1, −*y*+1, −*z*+1; (v) −*x*+2, −*y*+1, −*z*+1; (vi) −*x*+2, −*y*, −*z*+2; (vii) *x*, *y*+1, *z*−1; (viii) −*x*+1, −*y*, −*z*+2.